Title: Systemic Calcitonin Gene-Related Peptide (CGRP) modifies auditory and vestibular endorgan electrical potentials, and increases auditory and vestibular hypersensitivities: Implications for vestibular migraine

Abbreviated Title: CGRP's effect on inner ear endorgan and behavior

Authors: Shafaqat M. Rahman[1], Benjamin Liang[1], Stefanie Faucher[1], Elana Fine[1], Raajan Jonnala[1], Joseph C. Holt[2,3], Choongheon Lee[3], Anne E. Luebke[1,2*]

Affiliations:

[1]University of Rochester, Department of Biomedical Engineering, Rochester, NY 14627

[2]University of Rochester Medical Center, Department of Neuroscience, Del Monte Institute of Neuroscience, Rochester, NY 14642

[3]University of Rochester Medical Center, Department of Otolaryngology, Rochester, NY 14642

*Corresponding author: Anne E. Luebke, aluebke@ur.rochester.edu

Number of Pages: 21

Number of Figures: 3

Number of Tables: 0

Number of words for Abstract: 225

Number of words for Introduction: 343

Number of words for Discussion: 617

Conflict of interest statement: The authors declare no competing financial interests.

Acknowledgments: This work was fully supported by NIH R01DC017261.

Abstract:

Migraine is a severe and chronic neurological disorder that affects ~18% of people worldwide, the majority being female (3:1). It is characterized by recurrent, debilitating headaches and heightened sensory sensitivities. People with migraine may also experience a heightened motion sensitivity that leads to episodes of vertigo and imbalance, termed vestibular migraine (VM). Calcitonin Gene-Related Peptide (CGRP) is implicated in migraine and is believed to act on brain meninges, midbrain, or brainstem, and CGRP-based therapeutics have shown efficacy for migraine treatment. CGRP also signals at efferent synapses of the cochlea and vestibular endorgans, but it is unclear if exogenous CGRP can modulate inner ear function and cause heightened behavioral responses consistent with VM. In C57BL/6 mice, we tested if intraperitoneally (IP) delivered CGRP can modulate endorgan potentials to sound [via auditory brainstem responses (ABRs)] and jerk stimulus [via vestibular sensory evoked potentials (VsEPs)]. We also assessed behavioral measures of phonophobia [acoustic startle reflex (ASR)] and imbalance [postural sway-center of pressure (CoP)] after IP CGRP, and observed female mice exhibit heightened sensitivities to IP CGRP in all assays. Male mice showed similar auditory sensitivity and endorgan effects, but no postural sway changes. In conclusion, we show that systemically delivered CGRP modulates the nerve activity of the auditory and vestibular endorgans and elicits behavioral effects that are consistent with symptoms in a disorder like VM.

Significance statement:

Calcitonin Gene-Related Peptide (CGRP) has been implicated in migraine, and CGRP-based therapeutics have shown efficacy in the treatment of migraine headaches. CGRP is also present in efferent synapses of the inner ear, but we questioned if increases in systemic CGRP can act directly on inner ear endorgans and modify corresponding behavioral responses. In this study, we determined systemic CGRP changes cochlear and vestibular endorgan potentials and produces behaviors suggestive of phonophobia and postural sway. Peripheral changes in auditory and vestibular compound action potentials following systemic CGRP administration suggest CGRP can act directly on the inner ear, which provides a basis for CGRP's involvement in migraine with vertigo and as a therapeutic target.

50

51 **Introduction:**

52 Migraine is a debilitating chronic neurological disorder that is listed by the World Health Organization
53 (WHO) as the most debilitating neurological disorder worldwide and is estimated to affect 18% of
54 women and 6% of men (Goadsby, Lipton, and Ferrari 2002; Lipton et al. 2007). About 42% of people
55 with migraine have a vestibular component causing balance problems and dizziness (Kuritzky, Toglia,
56 and Thomas 1981; Neuhauser et al. 2001; Neuhauser 2007, 2009), termed vestibular migraine (VM).
57 VM is a major cause of vertigo in dizziness clinics (Kayan and Hood 1984) and patients with migraine,
58 and especially VM, exhibit a heightened sense of sound and motion (Ashkenazi et al. 2009; Lopez-
59 Escamez et al. 2014). Despite migraine and VM's prevalence, the pathophysiology remains uncertain
60 (Lempert et al. 2022; Lempert et al. 2012).

61

62 Calcitonin gene-related peptide (CGRP) is intensively studied for its role in migraine's sensory
63 hypersensitivities (Russo 2015). CGRP levels are elevated during migraine, and normalization of
64 CGRP levels is associated with the relief of headache pain which is thought to act at either brain
65 meninges or the trigeminal system (Goadsby, Lipton, and Ferrari 2002; Juhasz et al. 2005; Lassen et
66 al. 2002). CGRP also signals at efferent synapses of the cochlea and vestibular endorgans, so we
67 questioned if elevated CGRP levels in migraine could directly affect the inner ear. To that end, we
68 modeled the increase in CGRP during migraine by a systemic intraperitoneal (IP) injection to determine
69 if systemic CGRP can modulate activity of these endorgans (Dickerson et al. 2016; Luebke et al. 2014;
70 Maison et al. 2003). We also questioned if increases in systemic CGRP can cause behaviors
71 suggestive of heightened auditory and vestibular sway consistent with VM.

72

73 In this study, we tested wildtype C57BL/6 mice to determine if there is a change in endorgan potentials
74 to sound (measured using auditory brainstem responses - ABRs) and jerk stimulus (measured using
75 vestibular stimulus evoked potentials - VsEPs) after a CGRP injection. We also assessed
76 corresponding behavioral measures of phonophobia (acoustic startle reflex – ASR) and imbalance
77 (postural sway/center of pressure - CoP) after systemic CGRP injection.

78

79 **Methods:**

80 Animals: C57BL6/J mice were obtained from Jackson Laboratories (JAX #664) and were housed under
81 a 12-hour day/night cycle under the care of the University Committee on Animal Resources (UCAR) at
82 the University of Rochester. Mice were housed together in cages (5 mice per cage) with *ad libitum*
83 access to food, water, and bedding material. A total of 74 mice (37F/ 37M) were used for these studies,
84 which were powered sufficiently to detect male/female differences. Before experimentation, mice were
85 equilibrated in the testing room controlled for an ambient temperature between 22-23°C for at least 30
86 minutes, and remained in this room until completion of experiments. Injections occurred after the
87 equilibration period. Mice used during behavioral experiments were returned to the vivarium, while mice
88 used for ABR/VsEP experiments were euthanized after testing. Mice tested were between 2.3 - 6
89 months of age. This age range in mice correlates to 20-30 years in humans, which is within the age
90 range that patients develop migraine symptoms (Lessem 2018). All animal procedures were approved
91 by the University of Rochester's IACUC committee and performed in accordance with NIH standards.

92

93 VsEP and ABR Protocol: C57BL/6 mice were anesthetized with IP urethane/xylazine (1.2 g/kg/20
94 mg/kg). VsEP and ABR recording methods have been described in detail elsewhere (Lee, Holt, and
95 Jones 2017). Briefly, to record VsEP and ABR, subcutaneous electrodes were placed on the midline
96 over the nuchal crest (G1), behind the right pinna (G2), and on the hip (ground). A noninvasive head
97 clip was used to secure the mouse's head to an electromechanical shaker. During VsEPs, the shaker
98 delivered a transient (jerk) head translation in the naso-occipital axis (± X). To confirm the absence of
99 auditory responses during VsEP testing, a binaural forward masker (intensity: 92 dB SPL; bandwidth:
100 50~50 kHz) was presented with the use of a free-field speaker (FF1, TDT). For ABR recordings, the
101 same electrodes were used to record ABRs, which were evoked by a single rectangular voltage pulse
102 of 0.03 ms duration (corresponding to 33 kHz cut-off frequency). These click stimuli were presented via
103 a free-field speaker, which was the same driver for acoustic masking during the VsEP recording. A
104 noninvasive rectal thermometer or thermistor was used to monitor the animals' core temperature at
105 38.0 ± 0.2°C. The standard signal averaging technique described in previous studies (Lee, Holt, and

106 Jones 2017) was used to record both VsEP and ABR, as shown in **Fig. 1A**. Recordings of both VsEP
107 and ABR were made in a soundproof booth. Both VsEPs at maximal intensity +6 dB re: 1 g/ms and
108 ABRs at maximal intensity 100 dB SPL, were recorded as a stable baseline before a single IP injection
109 of either vehicle control (PBS) or 0.1 mg/kg CGRP was given. Control amplitude and latencies are
110 depicted as the averages of the 2-3 measurements taken during baseline before injection. Following
111 single IP injection of either vehicle or CGRP, VsEP and ABR recordings were continuously measured
112 where significant shifts in VsEP and ABR responses were first observed in 10 mins and reaching a
113 plateau within 15 mins of drug injection (post-CGRP; data not shown). Thus, amplitudes and latencies
114 depicted as post-saline/post-CGRP are averages of the 2-3 measurements taken after 20-30 min post-
115 injections.
116
117 Drug administration: Injections were performed intraperitoneally (IP) with a fine gauge (30ga) insulin
118 syringe. Dulbecco PBS served as the vehicle control. IP CGRP was prepared at 0.1 mg/kg (rat α-
119 CGRP, Sigma). Injection volumes were calibrated so that each animal received 1 injection per testing
120 day at ~100 ul. For behavioral experiments, mice were tested ~20 minutes after IP delivery of either
121 vehicle or CGRP.
122
123 Behavioral test of phonophobia: Acoustic startle reflex (ASR)
124 We used the acoustic startle response (ASR) to assess heightened sound sensitivity as a mouse
125 surrogate behavior for phonophobia. Experiments were conducted within a sound-attenuating room
126 (IAC, Bronx, NY) with Sonex foam lined walls. Mice were placed individually in a wire-mesh cage that
127 is 5 cm wide, 7 cm long, and 4 cm high, and having free sound penetration. The testing cage was
128 oriented so that the mouse's head faced a Tucker Davis ES2 electrostatic speaker (Masker Speaker)
129 located 46 cm directly in front of the mouse's head (60dB BBN). The startle speaker was a Radio
130 Shack tweeter that was suspended 15 cm above the mouse (80-130 dB). The acoustic startle speaker
131 and its supports, the pedestal, acrylic shelf, and the table on which the apparatus was placed were all
132 covered with echo absorbing foam and carpeting. Force of the acoustic startle response (ASR) was
133 transduced by an accelerometer and amplitude scored as integrated root mean square voltage for 100

134 ms after delivery of the ASR. Experimental stimuli were controlled, and responses were recorded
135 using custom MATLAB (MathWorks) software. We tested acoustic startle series in quiet and in noise.
136 There were 12 conditions in this session, with startle stimuli ranging from 80 to 130 dB SPL, and
137 delivered either in silence or in a continuous background noise. When present, background noise was
138 on for the duration of the inter-trial interval and broadcasted from the masker speaker, as shown
139 schematically in **Fig. 2**.
140
141 Behavioral test of postural sway
142 Postural sway was examined using the center of pressure (CoP) test which acts as a mouse surrogate
143 behavior for static imbalance. Mice were weighed and placed on a force plate designed to measure
144 forces in the X, Y, Z and moments in the XY, YZ, and XZ directions. We used the AMTI Biomechanics
145 Force platform (model HEX6x6) and AMTI automated acquisition software to obtain forces and
146 moments and then MATLAB code was used to calculate CoP measures based on a confidence ellipse
147 enclosing 95% of the CoP trajectory values recorded in a single trial. During a given test, mice were
148 first allowed to freely maneuver on the force plate for 2-5 minutes to acclimate to the novel
149 environment. An accessory plexiglass guard was placed around the force plate to prevent mice from
150 moving off the test plate. After acclimation, ~ 10 baseline trials were taken of mice with each trial
151 indicating a CoP area (resolution per CoP measurement: 300 samples per second). These trials were
152 taken when the mouse showed no movement and its four paws were touching the force platform. To
153 assess the effect of a vestibular challenge (VC), mice were then subjected to a constant orbital rotation,
154 125 rpm for 5 minutes, and were placed back onto the force platform. After a five-minute recovery
155 period, an additional 10 trials were recorded of the mouse's sway to determine post-VC effects on CoP
156 as schematized in **Fig. 3**. Mice were first tested after systemic delivery of IP vehicle (20 min after
157 injection), with sway measured before and after the VC. Four days after vehicle testing, the same mice
158 were injected with IP CGRP and were tested again 20 minutes after injection (timing correlated with
159 endorgan potential changes). While systemic CGRP's effect is believed to dissipate two to three hours
160 post–injection, we retested after four days to eliminate any residual dizziness due to VC or lingering
161 CGRP effects. We staggered sequence of IP injections in some animals by injecting CGRP followed by

162 vehicle testing on the next day. We also injected vehicle 2x to assess test/retest reliability and saw no
163 differences. Unreasonably large CoP values (> 15 cm^2) suggested mice were either moving during the
164 trial or that they were at the edge of the force plate, and those values were excluded based on a 10%
165 ROUT analysis (GraphPad Prism 9.0). Even with values excluded, a minimum of eight different 95%
166 ellipses were computed per mouse in a given testing condition. Furthermore, we excluded mice that
167 were outliers by running a second 10% ROUT on averaged CoPs per testing condition.
168
169 Statistical Analyses
170 All statistical analyses were conducted in GraphPad Prism 9.5. Analyses were conducted
171 separately in females and males. Repeated measure ANOVA (RM-ANOVA) and paired t-tests were
172 the primary statistical tools. Tukey post hoc analysis was used to assess treatment differences in
173 females or males, and Bonferroni post hoc analysis was used to assess treatment differences between
174 sexes. Significance was set at $p < 0.05$ for all analyses.
175
176 **Results:**
177 IP CGRP's Effects on ABR:
178 Representative traces are shown for ABR recordings in female and male C57BL6/J mice **(Fig. 1B-1C)**.
179 Female control ABR amplitudes (n = 6) were computed to be 3.60 ± 0.22 μV but were increased to 4.28
180 ± 0.25 μV after IP CGRP (one-tailed paired t-test; t, df = 3.99, 5; p = 0.005). Likewise, a similar trend
181 was observed in males as their control amplitudes (n = 7) were computed to be 4.31 ± 0.5 μV and
182 increased to 4.66 ± 0.44 μV after IP CGRP (one-tailed paired t-test; t, df = 1.94, 6; p = 0.05) **(Fig. 1F)**.
183 Wave 1 ABR amplitudes were normalized so that post-CGRP measurements highlight the change in
184 amplitude from their respective control measurements (Δ wave1 amplitude) **(Fig. 1G)**. When sexes are
185 pooled (n = 13), a significant Δ increase of 0.50 ± 0.13 μV was observed in wave 1 amplitudes due to
186 IP CGRP (one-tailed paired t-test**;** t, df = 3.9,12**;** p = 0.001). Wave 2-1 ABR latencies were calculated
187 as the difference between P2 and P1 latencies for control and post-CGRP; however, no differences
188 were observed in latency differences **(Fig. 1H).** A separate group of mice was tested for the effects of

189 PBS as the vehicle (data not shown, n = 4), but no differences were seen in Δ wave1 amplitude or
190 latency differences between control and post-vehicle (Δ wave1 amplitude $_{vehicle - control}$ = -0.19 ± 0.21 μV).
191
192 IP CGRP's Effects on VsEPs:
193 Similar to ABR tests, representative traces are shown for VsEP recordings in females and males (**Fig.**
194 **1D-1E).** Female P1-N1 VsEP control amplitudes (n = 6) were computed to be 0.68 ± 0.06 μV and were
195 reduced to 0.55 ± 0.06 μV after IP CGRP (one-tailed paired t-test; t, df = 1.96, 5; t (p = 0.054)) **(Fig. 1I)**.
196 Likewise, male P1-N1 VsEP control amplitudes (n = 8) were computed to be 0.95 ± 0.10 μV but were
197 reduced significantly to 0.76 ± 0.10 μV after IP CGRP (one-tailed paired t-test; t, df = 3.00, 7; p < 0.01).
198 P1-N1 amplitudes were normalized so that post-CGRP measurements highlight the change in
199 amplitude from their respective control (Δ P1-N1 amplitude), and both sexes were additionally pooled
200 (**Fig. 1J**). When pooling all animals (n = 14), a significant Δ reduction of -0.16 ± 0.04 uV in P1-N1
201 amplitude is observed due to IP CGRP (one-tailed paired t-test**;** t, df = 3.65, 13**;** p = 0.002).
202
203 P1, N1, and P2 latencies were also assessed for VsEPs, and these latencies are depicted as mean ±
204 SEM for females and males during control and post-CGRP tests **(Fig. 1K).** While no significant
205 differences were observed due to IP CGRP, modest delays in P1 were observed due to IP CGRP in
206 either sex. IP CGRP increased female P1 by 26.6 microseconds and male P1 by 22.5 microseconds
207 compared to P1 control latencies. IP CGRP also increased female N1 by 30 microseconds but had no
208 effect on Male N1. However, these latency changes were not statistically significant. Comparatively in
209 mice treated with IP vehicle, no significant P1-N1 amplitude or latency differences were observed
210 between control and post-vehicle VsEP (Δ P1-N1 amplitude $_{vehicle - control}$ = -0.03 ± 0.08 μV).
211
212 CGRP's effect on sound sensitivity
213 Our sound sensitivity measure in the mouse model makes use of the acoustic startle response (ASR) in
214 quiet and in background noise. Mice were assessed for the effects of IP CGRP as compared to IP
215 vehicle on their baseline. The ASR experimental setup is illustrated in **Fig. 2 A** (quiet) and **Fig. 2D**
216 (background noise 60 dB). In both IP vehicle and IP CGRP injected animals, an increase in ASR was

217 detected with increasing loudness of the startle stimulus (ES). All animals tested exhibited robust
218 startle responses (*n* = 6F/ 6M). When ASR was tested after IP CGRP injection and compared to IP
219 vehicle, all animals exhibited reduced ASR thresholds in both quiet and noise. IP CGRP significantly
220 increased sound sensitivity to the startle stimulus in quiet (**Fig. 2 B, C**) and in background noise (**Fig. 2**
221 **E, F**) in both female and male mice at all sound levels ($p < 0.0001$ quiet, $p < 0.001$ in noise).
222
223 CGRP's and VC's effects on Postural Sway
224 Mice were assessed for postural sway by determining center of pressure (CoP) ellipse area. An
225 experimental timeline is shown in **Fig. 3A**. Twenty minutes after delivery of IP vehicle and without a
226 vestibular challenge (VC), group averages of 95% ellipse areas were computed to be 0.5 ± 0.06 cm^2 for
227 females and 0.4 ± 0.04 cm^2 for males **(Fig. 3B and C).** For comparison, a deadweight (toy mouse) was
228 also measured on the force platform, and its average 95% ellipse area was computed to be 0.02 ±
229 0.0005 cm^2 **(Fig. 3D).** A different cohort of mice (*n* = 10F/ 10M) was assessed for a test-retest of 95%
230 ellipse areas after IP vehicle treatment, and testing occurred four days apart. A 2-way repeated
231 measures ANOVA with Bonferroni post-hoc analysis indicated no significant differences in either sex
232 during the test-retest for females (mean difference = 0.10 ± 0.3 cm^2) or for males (mean difference = -
233 0.14 + 0.3 cm^2) ($p > 0.99$ for either sex). In either sex, 2-way ANOVAs with Tukey post hoc analyses
234 were used to assess the factors of CGRP and VC on 95% CoP ellipse areas in mice (n = 14F/ 10M)
235 **(Fig. 3E).** Differences were seen in females due to IP CGRP (F (1.00, 13.00) = 4.77, p = 0.05) and the
236 VC (F (1.00, 13.00) = 4.49, p = 0.05). In females after IP vehicle, the VC induced higher CoP ellipse
237 compared to pre-VC trials (p = 0.02) as shown in **Fig. 3F**. When comparing pre-VC trials, IP CGRP
238 induced increases in female CoP areas by 0.94 ± 0.23 cm^2 compared to IP vehicle (p = 0.003) as seen
239 in **Fig. 3G.** Females also had 0.96 ± 0.15 cm^2 higher CoP areas than males based on a separate 2-way
240 ANOVA assessing sex differences in pre-VC, CGRP and post-VC, CGRP results (p = 0.001).
241 The major and minor axes of 95% ellipse areas were also analyzed with 2-way ANOVAs across
242 the factors CGRP and VC (**Fig. 3H and I**). The major and minor axes lengths serve as correlates for
243 anteroposterior (AP) and mediolateral (ML) sway magnitudes. A 2-way RM ANOVA on major axes
244 indicated significant effects in females due to IP CGRP (F (1.00, 13.00) = 5.59; p = 0.03) and VC (F

245 (1.00, 13.00) = 5.41; p = 0.04) whereas these effects were not observed in males. In comparison,
246 ANOVAs that analyzed minor axes indicated a VC effect in only females (F (1.00, 13.00) = 7.46; p =
247 0.02). Tukey post-hoc indicated IP CGRP induced larger AP ellipse lengths by 0.49 + 0.10 cm in
248 females compared to their IP vehicle trials (p = 0.001). Also, in IP vehicle-treated females, there was an
249 increase in AP ellipse lengths during the post-VC test versus pre-VC (p = 0.02). IP CGRP-treated
250 females exhibited greater AP lengths compared to males during pre-VC testing by 0.57 + 0.08 cm (p <
251 0.001). ML lengths increased after the VC in IP vehicle-treated females (p = 0.02), and IP CGRP-
252 treated females had higher ML ellipse lengths compared to their IP vehicle response (p = 0.007). No
253 other significant changes were observed in AP and ML sway.
254
255 **Discussion:**
256 Using electrophysiological techniques (ABR/VsEP), we observed that intraperitoneally delivered
257 CGRP modulates endorgan function in the inner ear with a maximum ~20- 30 minutes after injection.
258 Exogenous CGRP increases wave 1 amplitudes of the ABR but reduces VsEP P1-N1 amplitudes,
259 suggesting at least one action of systemic CGRP is at the efferent signaling sites of the auditory and
260 vestibular periphery. We did not characterize wave 2 and later peaks, as we were primarily interested in
261 wave 1/P1-N1 as an indicator of sensory processing changes at the periphery.
262 Furthermore, we observed that systemic CGRP - during this 20-to-30-minute timeframe -
263 increased sound sensitivity in male and female C57BL/6J mice, whereas it only increased postural
264 sway in females.
265 A few studies in animal models have provided additional evidence for CGRP's role in vestibular
266 dysfunction and sound sensitivity. Consistent with current VsEP results where we observed delays in
267 VsEP latencies due to systemic CGRP (though not statistically significant), the loss of αCGRP In
268 transgenic mouse lines significantly enhanced activation timing of the macular sensors through
269 changes at the endorgan level (Jones et al. 2018). Intracerebral-ventricular (ICV) injection of
270 nitroglycerin (NTG) caused impaired balance beam walking in rats, and immunohistochemistry
271 detected more CGRP expression in the vestibular nucleus of the NTG rat model than was observed in
272 controls. The administration of a CGRP-receptor antagonist (olcegepant-BIBN4096BS) was shown to

273 be effective in alleviating impaired balance beam walking (Zhang et al. 2020; Tian et al. 2022). In
274 addition, a recent study suggested CGRP has an excitatory role in the auditory nerve response, as
275 intra-cochlear CGRP infusion was shown to enhance spontaneous and sound-driven auditory nerve
276 activity in guinea pigs, in comparison to αCGRP-null mice where a loss of nerve activity excitation was
277 observed (Le Prell et al. 2021; Allen and Luebke 2017). Thus, the auditory nerve may be hyper-
278 sensitized to CGRP's effects during a migraine.

279 Peripheral effects of systemic CGRP administration on VsEP responses is somewhat surprising,
280 as the post-CGRP injection VsEP potentials were reduced and this result requires further examination
281 in future studies. However, this observation is relevant to VM, which is characterized by sensory
282 misintegration to stimuli, and thus reduced vestibular sensitivity that occurs concurrently with a
283 heightened auditory sensitivity may provide a basis for the occurrence of these symptoms.

284 Additionally, it is unclear why we did not find significant changes in males during postural sway
285 testing. While more males exhibited significant changes in their VsEP measures, we presume the lack
286 of CGRP-induced behavioral effects on sway may be due to other postural compensatory mechanisms
287 present in male mice. Yet, we did discover a robust sex difference when assessing mouse postural
288 sway, as female mice were much more affected than their male counterparts to injected CGRP.
289 Similar female-specific sexual dimorphism has been observed in other animal assays assessing
290 CGRP's effects in migraine but we are the first to show such differences in a preclinical, mouse
291 surrogate behavior for postural sway (Recober et al. 2009; Paige et al. 2022).

292 Small molecule blockers of the CGRP receptor ‘gepants’ have been shown to enter the
293 periphery, brainstem, and midbrain areas. Ongoing studies will determine if blocking CGRP receptor
294 signaling by small molecules (‘gepants”) or by larger monoclonal blocking antibodies (mAbs) - that may
295 or may not cross blood brain barrier (BBB), but are considered permeable to various peripheral ganglia
296 - can reduce these sound and imbalance sensitivities due to CGRP (Noseda et al. 2020; Tian et al.
297 2022; Zhang et al. 2020). The current evidence in favor of anti-CGRP mAbs for treating VM is
298 compelling, as a prospective observational cohort study over 18 months observed significant reduction
299 in vertigo and headache frequency in fifty VM patients treated with various anti-CGRP mAbs (Russo et
300 al. 2023).

References:

Allen, Paul D., and Anne E. Luebke. 2017. 'Reflex Modification Audiometry Reveals Dual Roles for Olivocochlear Neurotransmission', *Frontiers in Cellular Neuroscience*, 11.

Ashkenazi, A., A. Mushtaq, I. Yang, and M. L. Oshinsky. 2009. 'Ictal and interictal phonophobia in migraine-a quantitative controlled study', *Cephalalgia*, 29: 1042-8.

Dickerson, I. M., R. Bussey-Gaborski, J. C. Holt, P. M. Jordan, and A. E. Luebke. 2016. 'Maturation of suprathreshold auditory nerve activity involves cochlear CGRP-receptor complex formation', *Physiol Rep*, 4.

Goadsby, P. J., R. B. Lipton, and M. D. Ferrari. 2002. 'Migraine--current understanding and treatment', *N Engl J Med*, 346: 257-70.

Jones, S. M., S. Vijayakumar, S. A. Dow, J. C. Holt, P. M. Jordan, and A. E. Luebke. 2018. 'Loss of alpha-Calcitonin Gene-Related Peptide (alphaCGRP) Reduces Otolith Activation Timing Dynamics and Impairs Balance', *Front Mol Neurosci*, 11: 289.

Juhasz, G., T. Zsombok, B. Jakab, J. Nemeth, J. Szolcsanyi, and G. Bagdy. 2005. 'Sumatriptan causes parallel decrease in plasma calcitonin gene-related peptide (CGRP) concentration and migraine headache during nitroglycerin induced migraine attack', *Cephalalgia*, 25: 179-83.

Kayan, A., and J. D. Hood. 1984. 'Neuro-otological manifestations of migraine', *Brain*, 107 (Pt 4): 1123-42.

Kuritzky, A., U. J. Toglia, and D. Thomas. 1981. 'Vestibular function in migraine', *Headache*, 21: 110-2.

Lassen, L. H., P. A. Haderslev, V. B. Jacobsen, H. K. Iversen, B. Sperling, and J. Olesen. 2002. 'CGRP may play a causative role in migraine', *Cephalalgia*, 22: 54-61.

Le Prell, Colleen G., Larry F. Hughes, David F. Dolan, and Sanford C. Bledsoe. 2021. 'Effects of Calcitonin-Gene-Related-Peptide on Auditory Nerve Activity', *Frontiers in Cell and Developmental Biology*, 9.

Lee, C., J. C. Holt, and T. A. Jones. 2017. 'Effect of M-current modulation on mammalian vestibular responses to transient head motion', *J Neurophysiol*, 118: 2991-3006.

Lempert, T., J. Olesen, J. Furman, J. Waterston, B. Seemungal, J. Carey, A. Bisdorff, M. Versino, S. Evers, A. Kheradmand, and D. Newman-Toker. 2022. 'Vestibular migraine: Diagnostic criteria1', *J Vestib Res*, 32: 1-6.

Lempert, T., J. Olesen, J. Furman, J. Waterston, B. Seemungal, J. Carey, A. Bisdorff, M. Versino, S. Evers, and D. Newman-Toker. 2012. 'Vestibular migraine: diagnostic criteria', *J Vestib Res*, 22: 167-72.

Lessem, Sarah E. 2018. "QuickStats: Percentage of Adults Who Had a Severe Headache or Migraine in the Past 3 months, by Sex and Age Grou - National Health Interview Survey, United States, 2018." In *Morbidity and Mortality Weekly Report (MMWR)*, edited by National Center for Health Statistics.

Lipton, R. B., M. E. Bigal, M. Diamond, F. Freitag, M. L. Reed, W. F. Stewart, and Ampp Advisory Group. 2007. 'Migraine prevalence, disease burden, and the need for preventive therapy', *Neurology*, 68: 343-9.

Lopez-Escamez, J. A., J. Dlugaiczyk, J. Jacobs, T. Lempert, R. Teggi, M. von Brevern, and A. Bisdorff. 2014. 'Accompanying Symptoms Overlap during Attacks in Meniere's Disease and Vestibular Migraine', *Front Neurol*, 5: 265.

Luebke, A. E., J. C. Holt, P. M. Jordan, Y. S. Wong, J. S. Caldwell, and K. E. Cullen. 2014. 'Loss of alpha-calcitonin gene-related peptide (alphaCGRP) reduces the efficacy of the Vestibulo-ocular Reflex (VOR)', *J Neurosci*, 34: 10453-8.

348 Maison, S. F., R. B. Emeson, J. C. Adams, A. E. Luebke, and M. C. Liberman. 2003. 'Loss of alpha
349 CGRP reduces sound-evoked activity in the cochlear nerve', *J Neurophysiol*, 90: 2941-9.

350 Neuhauser, H. K. 2007. 'Epidemiology of vertigo', *Curr Opin Neurol*, 20: 40-6.

351 ———. 2009. '[Epidemiology of dizziness and vertigo]', *Nervenarzt*, 80: 887-94.

352 Neuhauser, H., M. Leopold, M. von Brevern, G. Arnold, and T. Lempert. 2001. 'The interrelations of
353 migraine, vertigo, and migrainous vertigo', *Neurology*, 56: 436-41.

354 Noseda, R., A. J. Schain, A. Melo-Carrillo, J. Tien, J. Stratton, F. Mai, A. M. Strassman, and R.
355 Burstein. 2020. 'Fluorescently-labeled fremanezumab is distributed to sensory and autonomic
356 ganglia and the dura but not to the brain of rats with uncompromised blood brain barrier',
357 *Cephalalgia*, 40: 229-40.

358 Paige, C., I. Plasencia-Fernandez, M. Kume, M. Papalampropoulou-Tsiridou, L. E. Lorenzo, E. T.
359 David, L. He, G. L. Mejia, C. Driskill, F. Ferrini, A. L. Feldhaus, L. F. Garcia-Martinez, A. N.
360 Akopian, Y. De Koninck, G. Dussor, and T. J. Price. 2022. 'A Female-Specific Role for
361 Calcitonin Gene-Related Peptide (CGRP) in Rodent Pain Models', *J Neurosci*, 42: 1930-44.

362 Recober, A., A. Kuburas, Z. Zhang, J. A. Wemmie, M. G. Anderson, and A. F. Russo. 2009. 'Role of
363 calcitonin gene-related peptide in light-aversive behavior: implications for migraine', *J Neurosci*,
364 29: 8798-804.

365 Russo, A. F. 2015. 'Calcitonin gene-related peptide (CGRP): a new target for migraine', *Annu Rev*
366 *Pharmacol Toxicol*, 55: 533-52.

367 Russo, Cinzia Valeria, Francesco Saccà, Simone Braca, Mattia Sansone, Angelo Miele, Antonio
368 Stornaiuolo, and Roberto De Simone. 2023. 'Anti-calcitonin gene-related peptide monoclonal
369 antibodies for the treatment of vestibular migraine: A prospective observational cohort study',
370 *Cephalalgia*, 43: 03331024231161809.

371 Tian, R., Y. Zhang, Q. Pan, Y. Wang, Q. Wen, X. Fan, G. Qin, D. Zhang, L. Chen, Y. Zhang, and J.
372 Zhou. 2022. 'Calcitonin gene-related peptide receptor antagonist BIBN4096BS regulates
373 synaptic transmission in the vestibular nucleus and improves vestibular function via
374 PKC/ERK/CREB pathway in an experimental chronic migraine rat model', *J Headache Pain*, 23:
375 35.

376 Zhang, Y., Y. Zhang, K. Tian, Y. Wang, X. Fan, Q. Pan, G. Qin, D. Zhang, L. Chen, and J. Zhou. 2020.
377 'Calcitonin gene-related peptide facilitates sensitization of the vestibular nucleus in a rat model
378 of chronic migraine', *J Headache Pain*, 21: 72.

379

380

381

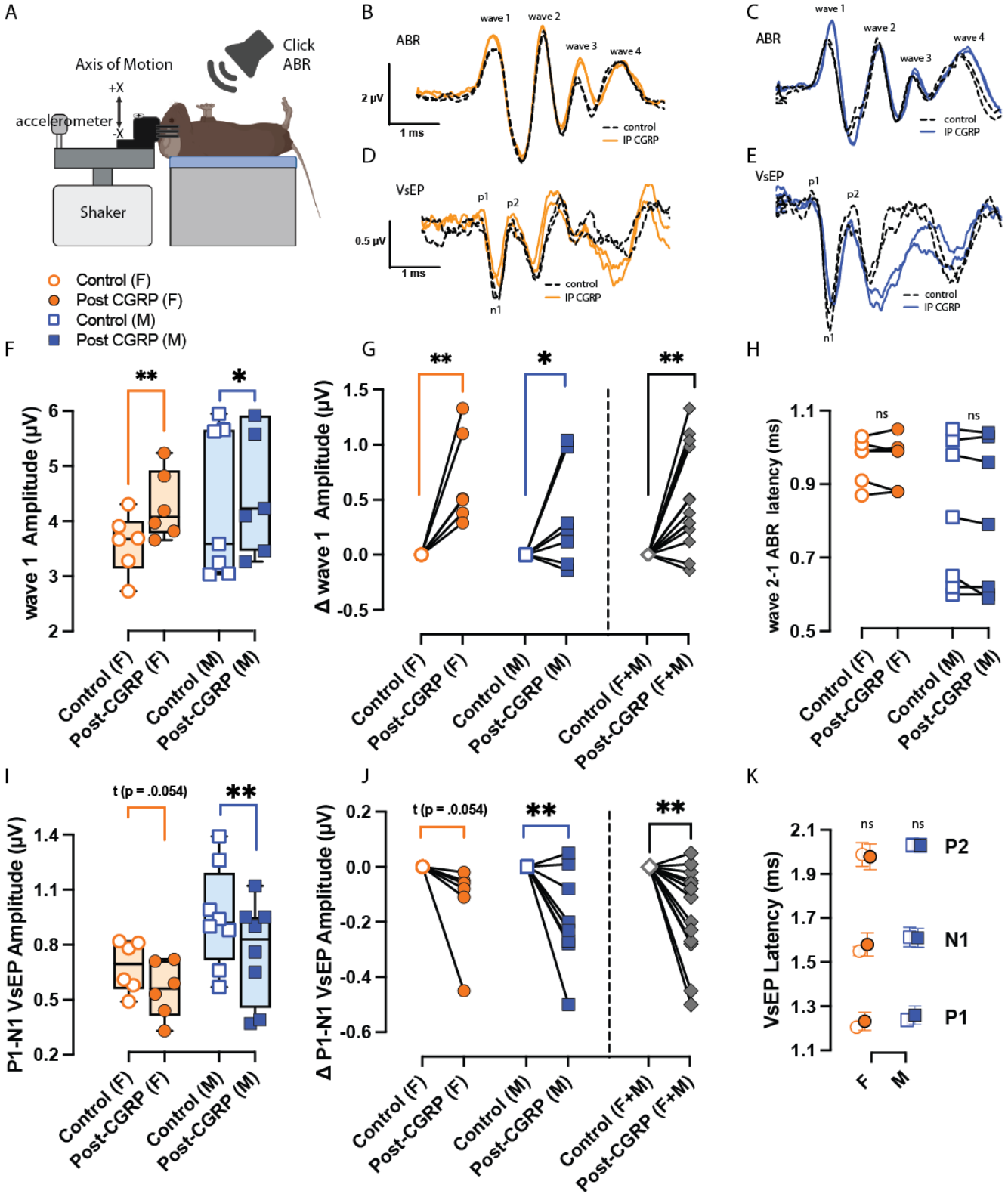
A
Axis of Motion
+X
-X
accelerometer
Shaker
Click
ABR
Control (F)
Post CGRP (F)
Control (M)
Post CGRP (M)
B
ABR
wave 1
wave 2
wave 3
wave 4
2 µV
1 ms
control
IP CGRP
C
ABR
wave 1
wave 2
wave 3
wave 4
control
IP CGRP
D
VsEP
p1
p2
n1
0.5 µV
1 ms
control
IP CGRP
E
VsEP
p1
p2
n1
control
IP CGRP
F
wave 1 Amplitude (µV)
Control (F)
Post-CGRP (F)
Control (M)
Post-CGRP (M)
G
Δ wave 1 Amplitude (µV)
Control (F)
Post-CGRP (F)
Control (M)
Post-CGRP (M)
Control (F+M)
Post-CGRP (F+M)
H
wave 2-1 ABR latency (ms)
ns
Control (F)
Post-CGRP (F)
Control (M)
Post-CGRP (M)
I
P1-N1 VsEP Amplitude (µV)
t (p = .0.054)
Control (F)
Post-CGRP (F)
Control (M)
Post-CGRP (M)
J
Δ P1-N1 VsEP Amplitude (µV)
t (p = .0.054)
Control (F)
Post-CGRP (F)
Control (M)
Post-CGRP (M)
Control (F+M)
Post-CGRP (F+M)
K
VsEP Latency (ms)
ns
P2
N1
P1
F
M

Fig. 1

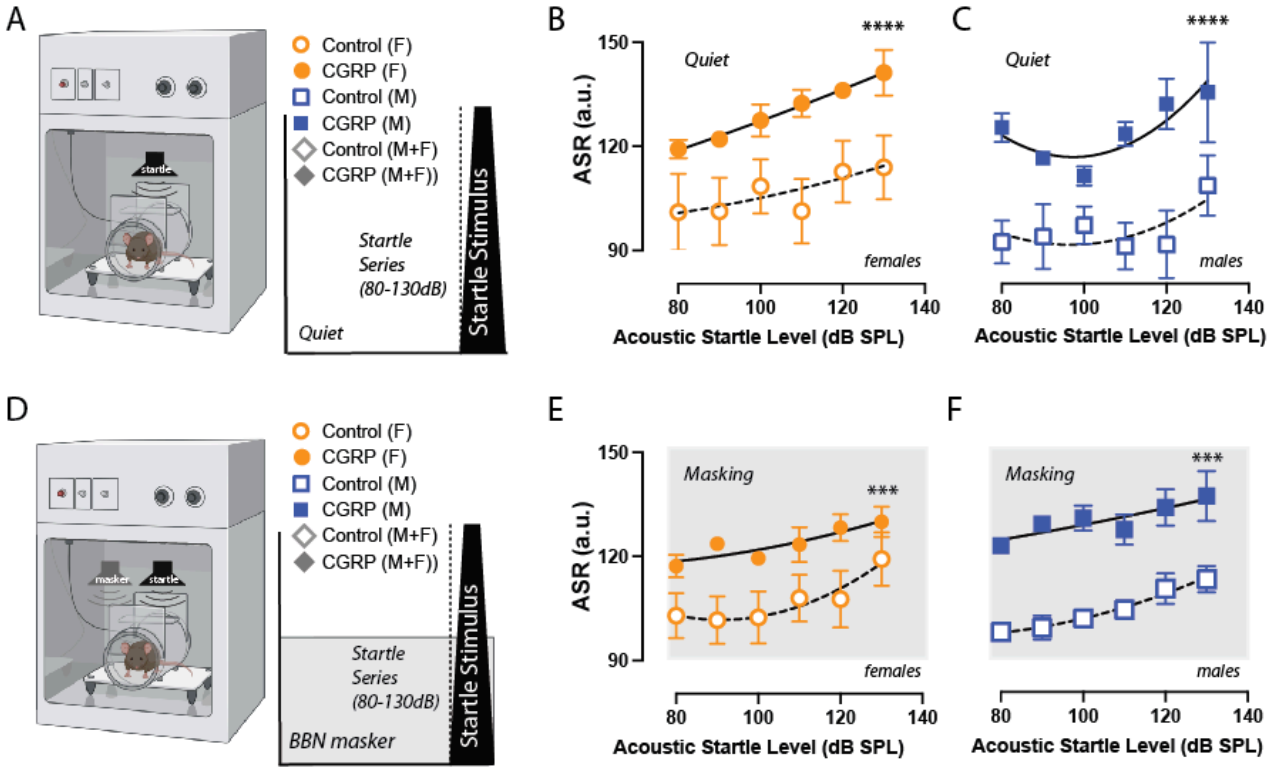
A
Control (F)
CGRP (F)
Control (M)
CGRP (M)
Control (M+F)
CGRP (M+F))
Startle Series (80-130dB)
Quiet
Startle Stimulus
B
Quiet
****
ASR (a.u.)
150
120
90
females
80
100
120
140
Acoustic Startle Level (dB SPL)
C
Quiet
****
males
Acoustic Startle Level (dB SPL)
D
Control (F)
CGRP (F)
Control (M)
CGRP (M)
Control (M+F)
CGRP (M+F))
Startle Series (80-130dB)
BBN masker
Startle Stimulus
E
Masking
***
ASR (a.u.)
150
120
90
females
Acoustic Startle Level (dB SPL)
F
Masking
***
males
Acoustic Startle Level (dB SPL)

Fig. 2

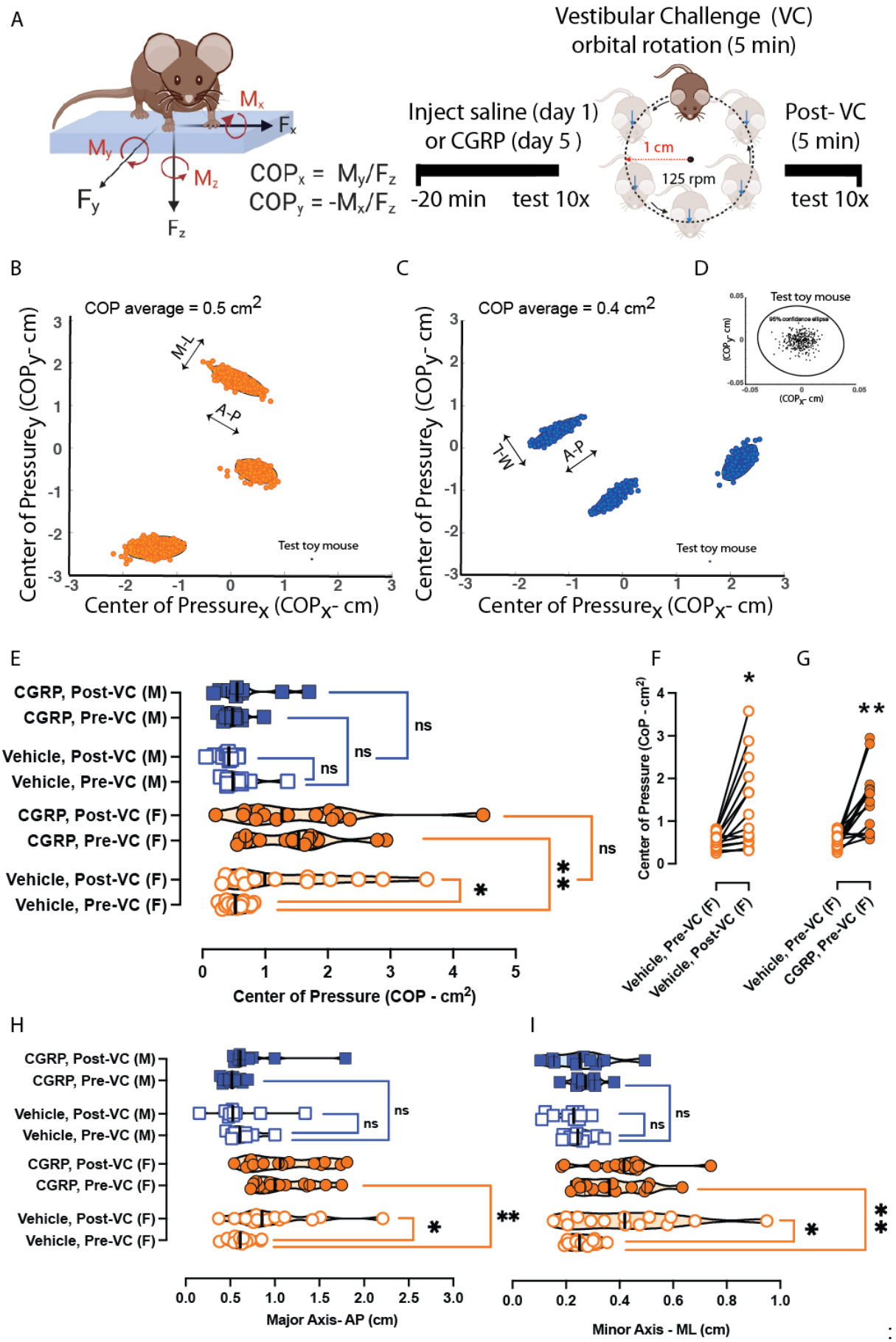
A
Vestibular Challenge (VC)
orbital rotation (5 min)
Inject saline (day 1)
or CGRP (day 5)
Post- VC
(5 min)
1 cm
125 rpm
-20 min
test 10x
test 10x
COPx = My/Fz
COPy = -Mx/Fz
B
C
D
COP average = 0.5 cm2
COP average = 0.4 cm2
Test toy mouse
Center of Pressure (COPx- cm)
Center of Pressure (COPy- cm)
E
F
G
CGRP, Post-VC (M)
CGRP, Pre-VC (M)
Vehicle, Post-VC (M)
Vehicle, Pre-VC (M)
CGRP, Post-VC (F)
CGRP, Pre-VC (F)
Vehicle, Post-VC (F)
Vehicle, Pre-VC (F)
ns
Center of Pressure (COP - cm2)
Center of Pressure (CoP - cm2)
H
I
Major Axis- AP (cm)
Minor Axis - ML (cm)

Fig. 3

391 **Figure Legends:**

392 **Fig. 1.** ***A,*** Schematic illustrating mouse setup for VsEP/ABR recordings captured during baseline
393 (control) and 20-30 minutes after intraperitoneal (IP) injections of either PBS vehicle or 0.1 mg/kg
394 CGRP in male (M) and female (F) C57BL6/J mice***. B-C,*** Representative click-evoked ABR waveforms -
395 in duplicate -were collected for ABR at a maximal intensity of 100 dB SPL, and waves were labeled
396 (wave1 – wave 4). ***D-E,*** Likewise, representative VsEP waveforms were collected at +6 dB re: 1 g/ms
397 having three, labeled response peaks (p1, n1, and p2). Orange and blue colors are used to distinguish
398 female and male tracings post-CGRP, respectively. The following symbols and colors are used: female
399 - orange, male - square, control - open, CGRP - closed. Sample sizes list - ABR (n = 6F/7M), VsEP (n =
400 6F/8M). ***G & J,*** Before/after plots indicate the change in amplitude post-CGRP compared to a control
401 response normalized to zero. ***F-G***, A significant increase is seen in wave 1 ABR amplitudes post CGRP
402 for female ($p = 0.005$), male ($p = 0.05$), and also when sexes are pooled ($p = 0.001$). ***I-J,*** For VsEPs, a
403 statistically significant decrease in P1-N1 VsEP amplitudes was seen in males ($p < 0.01$), a trend was
404 seen in females (t ($p = 0.054$)), and when sexes are pooled ($p = 0.002$). IP CGRP had no significant
405 effects on ***(H)*** ABR or ***(K)*** VsEP latencies. No amplitude or latency effects were observed in a separate
406 group of mice (*n* = 4) that were tested for baseline control and IP saline (not shown).

407

408 **Fig. 2. Systemic CGRP increases Acoustic Startle Responses (ASR) in both quiet and**
409 **background noise, suggesting increased sound sensitivity.** ***A,*** Schematic of startle stimulus
410 presented in otherwise quiet background conditions. ***B-C***, In female mice (***B***, n = 6), and male mice (***C***,
411 n=6), there were significant differences between vehicle and IP CGRP ASR measures in quiet
412 conditions ($p < 0.0001$). All mice were more sensitive to the same sound level of ASR stimulus after
413 being injected with CGRP. ***D,*** Schematic of startle stimulus embedded in continuous 60dB SPL
414 broadband background noise. ***E-F,*** ASR embedded in noise was also more sensitive to same sound
415 level after CGRP injection as shown for female mice (***E***, n = 6), male mice (***F***, n = 6), ($p < 0.001$). All
416 mice were more sensitive to the same level of ASR stimulus whether delivered in quiet or in BBN after
417 being injected with CGRP. Moreover, all mice showed ASR increases with sound level from 80 to
418 130dB SPL with near maximal startle is elicited by 130 dB SPL stimulus levels. Error bars are SEMs.

419

420 **Fig. 3. CGRP and VC's effects on postural sway.** Symbols and colors are depicted in a similar
421 scheme as previous figures. ***A,*** Timeline involved mice being assessed for effects of IP vehicle control
422 (saline) or IP CGRP on day 1 or day 5, respectively. A 5-minute orbital rotation (125 rpm for 5 minutes,
423 orbital radius = 1 cm) was used as the vestibular challenge, and mice were repeatedly tested (n =
424 14F/10M). ***B-C,*** Group 95% ellipse areas during pre-VC testing were computed to be 0.50 ± 0.06 cm^2
425 for females and 0.40 ± 0.04 cm^2 for males. ***D,*** A toy mouse was measured to be 0.02 ± 0.0005 cm^2 for
426 comparison with live animals. ***E,*** During IP CGRP pre-VC tests, females had higher 95% ellipse areas
427 compared to males by 0.96 ± 0.19 cm^2 ($p = 0.01$). ***F,*** Females exhibit greater sway after vestibular
428 challenge with vehicle injection ($p = 0.02$). ***G,*** Before-after plot shows during pre-VC testing in females,
429 IP CGRP caused increased 95% ellipse areas by 0.94 ± 0.23 cm^2 when compared to their IP vehicle
430 response ($p = 0.003$). ***H,*** For Pre-VC AP sway in females, IP CGRP increased AP ellipse lengths by
431 0.49 + 0.10 cm compared to IP vehicle ($p = 0.001$). An increase in female AP lengths was detected in
432 IP vehicle from pre-VC to post-VC, but this was trending ($p = 0.02$). ***I,*** For Pre-VC ML sway in females,
433 IP CGRP increased ML ellipse lengths by 0.12 + 0.03 cm compared to IP vehicle, ($p = 0.02$). In IP-
434 vehicle treated females, an increase (trend) in ML ellipse lengths is observed from pre-VC to post-VC
435 ($p = 0.02$), and IP CGRP-treated females had increased ML ellipse lengths compared to their vehicle
436 response by 0.12 + 0.03 cm ($p = 0.007$).